MICROBIOLOGY

Ruminococcin C, a promising antibiotic produced by a human gut symbiont

Steve Chiumento[1]*, Clarisse Roblin[2,3]*, Sylvie Kieffer-Jaquinod[4]*, Sybille Tachon[2], Chloé Leprètre[1], Christian Basset[1], Dwi Aditiyarini[1], Hamza Olleik[2], Cendrine Nicoletti[2], Olivier Bornet[5], Olga Iranzo[2], Marc Maresca[2], Renaud Hardré[2], Michel Fons[6], Thierry Giardina[2], Estelle Devillard[3], Françoise Guerlesquin[5], Yohann Couté[4], Mohamed Atta[1], Josette Perrier[2], Mickael Lafond[2†], Victor Duarte[1†]

A major public health challenge today is the resurgence of microbial infections caused by multidrug-resistant strains. Consequently, novel antimicrobial molecules are actively sought for development. In this context, the human gut microbiome is an under-explored potential trove of valuable natural molecules, such as the ribosomally-synthesized and post-translationally modified peptides (RiPPs). The biological activity of the sactipeptide subclass of RiPPs remains under-characterized. Here, we characterize an antimicrobial sactipeptide, Ruminococcin C1, purified from the caecal contents of rats mono-associated with *Ruminococcus gnavus* E1, a human symbiont. Its heterologous expression and post-translational maturation involving a specific sactisynthase establish a thioether network, which creates a double-hairpin folding. This original structure confers activity against pathogenic *Clostridia* and multidrug-resistant strains but no toxicity towards eukaryotic cells. Therefore, the Ruminococcin C1 should be considered as a valuable candidate for drug development and its producer strain *R. gnavus* E1 as a relevant probiotic for gut health enhancement.

INTRODUCTION

Over the coming decades, it has been estimated that millions of people will succumb to bacterial infections mainly due to the emergence of multidrug-resistant (MDR) strains (*1*, *2*). As a result, we urgently need to discover novel molecules and means to face this major threat. Bacteria constitute a treasure trove of multiple classes of natural antimicrobial compounds, one of which is ribosomally synthesized and posttranslationally modified peptides (RiPPs). RiPPs are biosynthesized from a genetically encoded precursor peptide, generally containing an N-terminal leader sequence and a C-terminal core peptide (*3*). Among these peptides, sactipeptides constitute a subclass of bacteriocins that emerged several years ago (*4*, *5*). Despite spectacular advances made with genomic tools, the sactipeptide subclass is currently limited to only six members (Fig. 1A) (*6*–*12*). Biosynthesis of most of these peptides relies on the expression of a gene cluster encoding at least one peptide precursor, a maturation enzyme named sactisynthase, which places posttranslational modifications, and two proteins, namely, an ABC transporter and a signal peptidase, which are involved in peptide export and signal peptide cleavage, respectively (Fig. 1B) (*13*).

In silico analysis of a 15-kb genomic fragment from the strictly anaerobic *Ruminococcus gnavus* E1 strain, a Gram-positive Firmicutes isolated from the feces of a healthy human, indicated a multi-operonic organization controlled by a two-component regulatory system (i.e., a regulon) (*14*). In addition to the genes involved in regulation, immunity, and export, the *rumC*-regulon includes five open reading frames (ORFs) (*rum*C1 to *rum*C5), which have been suggested to encode sactipeptide precursors (Fig. 1C), two ORFs (*rum*Mc1 and *rum*Mc2) thought to encode sactisynthases (fig. S1A), and one ORF (*rum*Pc) likely to encode Ruminococcin C (RumC) leader peptide-specific metallopeptidase from the M16 family (Fig. 1B) (*15*, *16*). Furthermore, previous works showed that *R. gnavus* E1 produces an anti-*Clostridium* substance in the rat gut in a trypsin-dependent manner (*17*). This substance was later partially purified, identified as RumC isoforms, and shown to be produced exclusively in vivo (*15*, *18*, *19*).

From a chemical maturation standpoint, sactisynthases introduce intramolecular thioether cross-links between cysteine sulfur and the unreactive α-carbon of a partner amino acid by a radical-based mechanism to produce sactipeptides (Fig. 1D) (*20*). All of the sactisynthases characterized so far have been classified in the Radical *S*-adenosyl-L-methionine (SAM) enzymes superfamily (*21*). Although their radical SAM domain is known to be directly involved in the formation of the thioether linkage, they all contain a C-terminal extension called SPASM (Subtilosin A/Pyrroloquinoline quinone/Anaerobic Sulfatase/Mycofactocin maturation enzymes) domain housing additional [4Fe-4S] clusters (*22*), for which the role is still under debate (*12*, *23*–*31*). While the number of sactipeptides is still limited, interesting biological properties have been found regarding their antimicrobial activity and their mode of action (*5*, *8*, *32*–*35*).

Here, we report the in vivo and in vitro production of the RumC1 sactipeptide and its functional and conformational characterizations. We highlight the strong antimicrobial activity against Gram-positive pathogens including MDR strains and the lack of toxic effect toward eukaryotic cells. Therefore, it has a valuable potential for drug development, and its producer strain *R. gnavus* E1 could be used as a powerful probiotic.

[1]Univ. Grenoble Alpes, CEA, CNRS, CBM-UMR5249, 38000 Grenoble, France. [2]Aix-Marseille Univ., CNRS, Centrale Marseille, iSm2, Marseille, France. [3]ADISSEO France SAS, Centre d'Expertise et de Recherche en Nutrition, Commentry, France. [4]Univ. Grenoble Alpes, CEA, INSERM, BGE U1038, 38000 Grenoble, France. [5]LISM, IMM, Aix-Marseille Univ., CNRS, Marseille, France. [6]Unité de Bioénergétique et Ingénierie des Protéines UMR7281, Institut de Microbiologie de la Méditerranée, Aix-Marseille Univ., CNRS, Marseille, France.
*These authors contributed equally to this work.
†Corresponding author. Email: mickael.lafond@univ-amu.fr (M.L.); victor.duarte@cea.fr (V.D.)

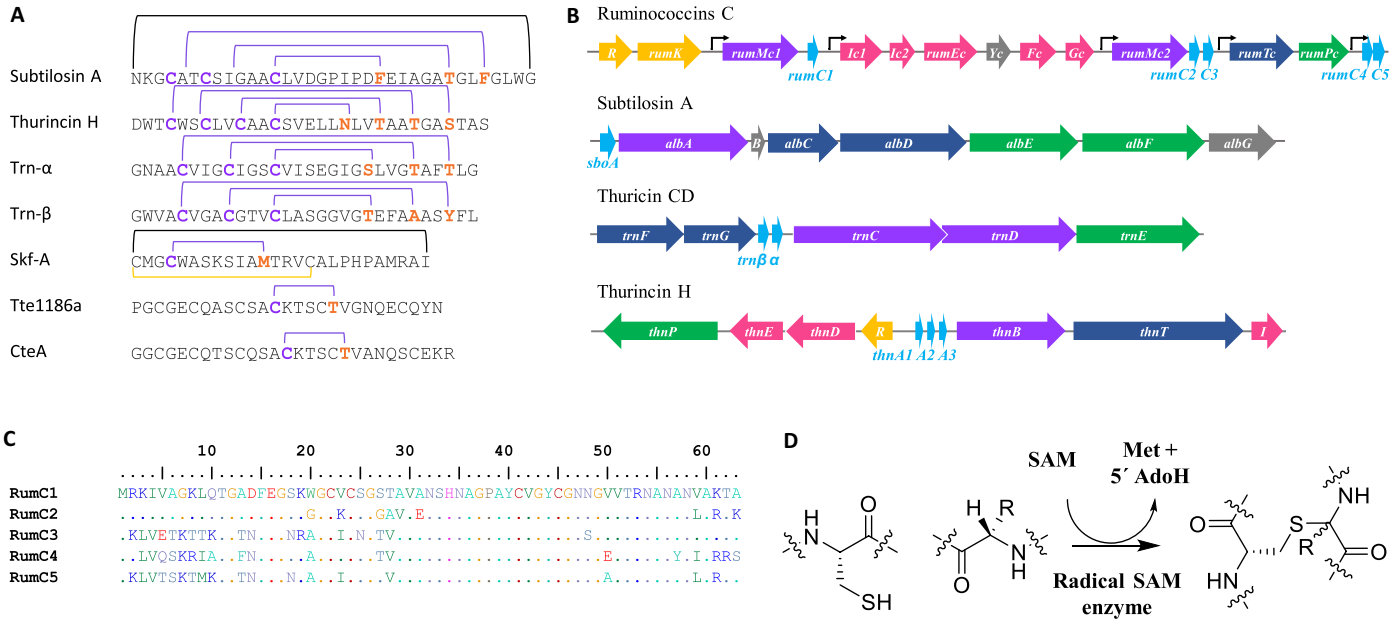

Fig. 1. Biosynthesis of sactipeptides. (**A**) Thioether network in previously described sactipeptides. Thioether bridges, disulfide bridges, and head-to-tail cyclization are indicated by purple, yellow, and black lines, respectively. (**B**) Gene regulon encoding ruminococcins C, subtilosin A, thuricin CD, and thurincin H. Purple, radical SAM enzymes; light blue, precursor peptides; dark blue, transporter systems; green, signal peptidases; yellow, response regulators; pink, immunity systems; and gray, genes of unknown function. (**C**) Alignment of the five RumC peptide isoforms. (**D**) Thioether bond formation in sactipeptides catalyzed by radical SAM enzymes.

RESULTS

In vivo production and purification of RumC1 from *R. gnavus* E1–monoassociated rats

Crost and co-workers (*18*) previously showed that when the digestive tract of axenic rats is colonized with *R. gnavus* E1 strain, the feces obtained and the cecal contents display an anti–*Clostridium perfringens* (anti-*Cp*) activity, which is genetically correlated with the *rumC*-regulon (Fig. 1B) (*15*). Consequently, we began our study by attempting to purify in vivo–produced RumC isoforms. After 12 days of colonization with *R. gnavus* E1, the feces were collected and the cecal contents of monoassociated rats were found to contain an anti-*Cp* substance (Fig. 2A). The expected RumC peptides are 44 amino acid strings after the removal of the supposed N-terminal leader sequence of 19 residues. An ultrafiltration approach based on expected molecular weights was used to enrich peptides of interest in the active fraction (Fig. 2A). The active soluble fraction was then submitted to three consecutives, and optimized chromatographic steps interleaved with desalting steps: cationic exchange, size exclusion, and hydrophobic C18 reversed-phase chromatography. Throughout the subsequent steps, the putative RumC-containing fractions were selected on the basis of an anti-*Cp* assay (Fig. 2A). Nano–liquid chromatography combined with mass spectrometry (LC-MS) analyses revealed a considerable enrichment of the five RumC isoforms in two consecutive fractions of the last purification step (Fig. 2, B and C), which displayed anti-*Cp* activity when combined (Fig. 2A). The masses of the five RumC peptides measured were consistently 8 Da less than their theoretical masses, as shown for in vivo and synthetically produced unmodified RumC1 peptide (Fig. 2, D and F). The iodoacetamide alkylation of the RumC-enriched fraction under reducing conditions failed to alter the observed masses of native RumC1 peptide, suggesting that the four cysteine residues are modified and most likely engaged in intramolecular bonds (Fig. 2E). Unlike the cross-links present in lantibiotics where thioether bridges are formed between the sulfur atom of a cysteine and the β-carbon of a corresponding residue, the thioether linkages in sactipeptides involve the α-carbon (*6*, *7*). This specificity is thought to result in opening of the thioether link during tandem MS (MS/MS) analyses, leading to the formation of a free cysteine and the dehydramino form of the partner amino acid, resulting in a two unit mass decrease (*36*). Higher-energy collisional dissociation–based MS/MS analyses of in vivo–produced RumC1 indicated that residues A12, N16, R34, and K42 are involved in thioether bridges (Fig. 3A and table S1). The same strategy was used to study the four remaining RumC peptides, and they were all found to contain four thioether bridges involving residues at the same positions as those identified in RumC1 (fig. S2).

RumC1 presents a novel thioether network

As thioether bridges open during MS/MS analyses, it is impossible to assign the different cysteine residues to their amino acid partners. Thus, we sought to establish a heterologous expression system allowing site-directed mutagenesis to accurately assign the residues involved in each thioether bridge. Furthermore, the in vitro production of RumC bacteriocins will facilitate future investigations including antimicrobial activity assays, structural, functional, and biophysical studies. Similar to the approach described by Himes and co-workers (*37*) for the production of subtilosin A in *Escherichia coli*, we established a protocol to produce heterologously the mature form of RumC1 (mRumC1), consisting of the leader and core peptide sequences. Here, the genes encoding the radical SAM enzyme RumMc1 and the RumC1 peptide were separately cloned into two different plasmids and co-expressed in the presence of *suf* genes (fig. S3, B and C, top and middle) (*38*). The observed mass of mRumC1 was in good agreement with the presence of four thioether linkages (Fig. 3B). Reductive alkylation of mRumC1 had no effect on its observed molecular

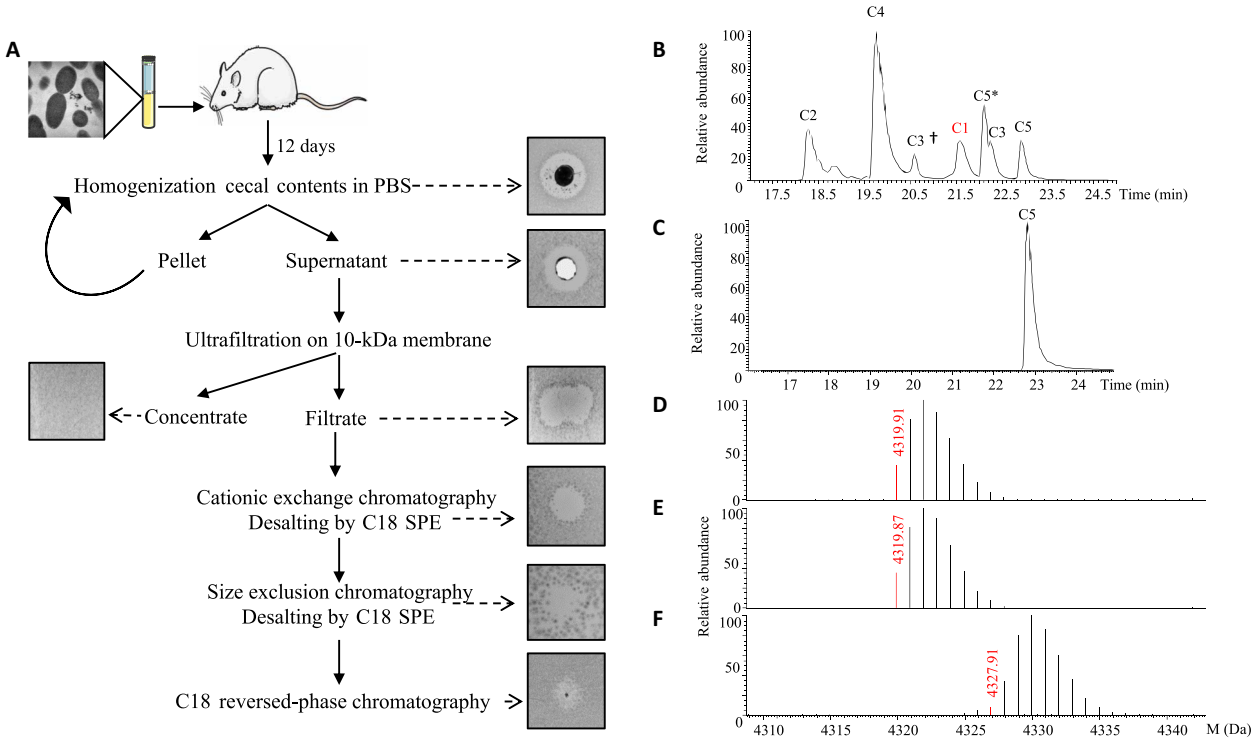

Fig. 2. Purification and characterization of the five RumC isoforms produced in vivo. (**A**) Protocol for extraction from cecal contents to obtain a purified mixture of RumCs. Fractions were selected on the basis of their anti-*Cp* activity throughout the purification steps. PBS, phosphate-buffered saline. (**B** and **C**) LC-MS analyses of the two fractions containing the different RumC (* and † indicate succinimide and deamidated forms of C5 and C3, respectively). RumC5 was present in two consecutive C18 reversed-phase fractions. (**D**) Deconvoluted mass spectrum of RumC1 eluted at 21.6 min in nano–LC-MS analyses. (**E**) Deconvoluted mass spectrum of RumC1 after dithiothreitol (DTT)/iodoacetamide treatment. (**F**) Deconvoluted mass spectrum of synthetic unmodified RumC1.

weight, thus suggesting that the four Cys residues in mRumC1 are involved in posttranslational modifications (Fig. 3C). LC-MS/MS analyses of mRumC1 confirmed the same four partner residues A, N, R, and K, corresponding to A12, N16, R34, and K42 in RumC1 purified from cecal contents (Fig. 3, A and B). In this sample, two peptide fragments, G(-23)-Y21 and A17-A44, were observed, corresponding to the N- and C-terminal parts, respectively, of mRumC1. Both of these fragments were detected with a 4-Da mass decrease (fig. S4, B and C). In good agreement with this observation, the C-terminal peptide, with a similar 4-Da loss of mass, was also detected in the RumC1-containing fraction from the in vivo preparation (fig. S4A). These important results suggest that mature RumC1 contains four thioether bridges, two each in the N- and C-terminal regions.

To identify the residues involved in each thioether bridge, four Cys to Ala mutants were designed: mRumC1-C3A, mRumC1-C5A, mRumC1-C22A, and mRumC1-C26A. All the mutants were produced and purified as described for mRumC1. To detect nonbridged cysteine residues, mutant mRumC1 samples were first treated with iodoacetamide under reducing conditions and then subjected to LC-MS/MS experiments. Analyses of the four single mutants revealed fairly complex peptide mixtures with many peptide fragments bearing alkylated cysteine residues. These data suggest that, during the maturation of mRumC1, the formation of a single thioether linkage may influence how the three other bridges form, making the structure highly labile. Nevertheless, interesting information can be gleaned from the fragmentation patterns of selected peptides present in the mixture. We focused our attention on the residues identified as partners of the four cysteines and for which the mass is either unmodified or presents a loss of 2 Da upon mutation of a single cysteine. MS/MS analysis of the Q(-10)-A20 peptide observed in the mRumC1-C3A mutant showed no mass loss on the N16 residue but a 2-Da decrease on A12. These data indicate that a thioether bridge forms between C5 and A12 and that the bridging partner for C3 is N16 (Fig. 3D, fig. S5A, and table S1). In good agreement, peptide F(-5)-A20 from the mRumC1-C5A mutant contains an unmodified A12 residue (Fig. 3D, fig. S5C, and table S1). In the mRumC1-C22A mutant, the fragmentation of the A17-A44 peptide revealed a 2-Da deficit for R34, whereas K42 was unmodified. These observations suggest that R34 and K42 are the partners of C26 and C22, respectively (Fig. 3D, fig. S5B, and table S1). Together, the MS/MS analyses of both wild-type and mutated mRumC1 peptides allowed us to propose a structural model for mature RumC1 in which the peptide is folded into two distinct structured domains both containing two thioether bridges; the two domains are separated by the strictly conserved AGPAY amino acid sequence present in all five RumC isoforms (Fig. 3E).

To establish the connectivity of the thioether rings, nuclear magnetic resonance (NMR) experiments were performed by using a ^{13}C-, ^{15}N–labeled mRumC1 sample after removal of the N-terminal leader sequence by trypsin. The [^{15}N, ^{1}H] heteronuclear single-quantum coherence (HSQC) spectrum gave well-dispersed peaks, with 39 of 42 backbone NH signals observed. The backbone NH signals for C26, G27, and N28 could not be observed. The sequential assignment was made on the basis of the backbone three-dimensional experiments,

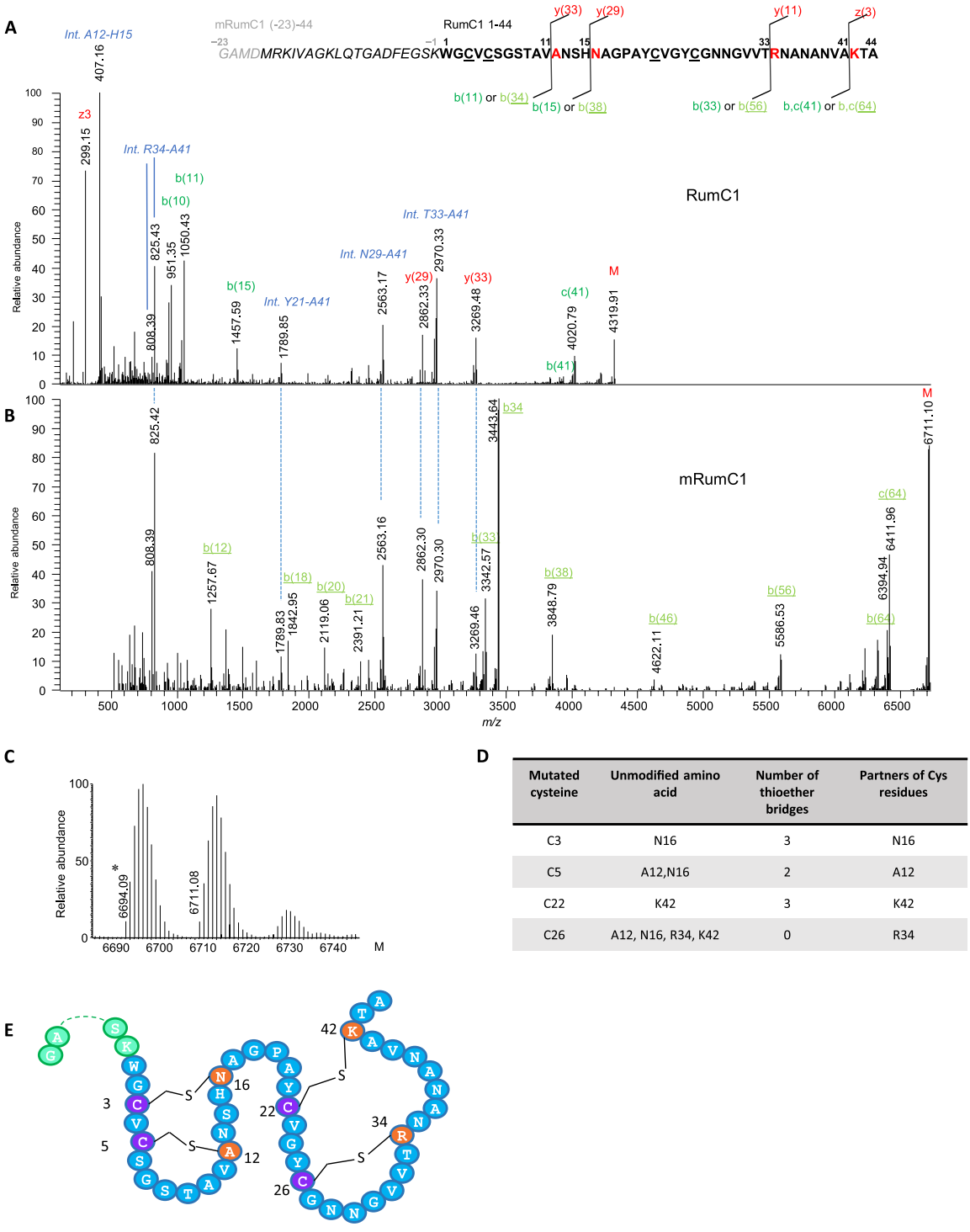

Mutated cysteine	Unmodified amino acid	Number of thioether bridges	Partners of Cys residues
C3	N16	3	N16
C5	A12,N16	2	A12
C22	K42	3	K42
C26	A12, N16, R34, K42	0	R34

Fig. 3. Tandem mass spectra of mature RumC1 peptide from in vivo and in vitro preparations and thioether network (see table S1 for theoretical and observed masses of interest). (**A**) Deconvoluted MS/MS spectrum of in vivo–matured RumC1 (1 to 44, bold sequence) showing prominent y/b and c/z fragments induced by breaking of the amide bonds preceding the residues bound to cysteines in thioether bridges. The very structured peptide produced high-intensity and unusual internal fragments (blue italics), particularly ANSH (A12-H15) and RNANANVA (R34-A41), corresponding to fragments located between two linked residues. (**B**) Deconvoluted MS/MS spectrum of the heterologously matured mRumC1 [containing leader peptide (italics) and four additional GAMD amino acids for cloning purposes (gray italics)], revealing the same characteristic fragmentation pattern. Peaks below 500 Da (identical for the y series of in vivo RumC1) are not shown to improve overall visibility. All masses considered are monoisotopic masses. M (last peak in each spectrum) corresponds to the nonfragmented peptide. (**C**) Deconvoluted MS spectrum of mRumC1 after DTT/iodoalkylation showing no mass increment. Mass of 6694.09 (ammonia loss) corresponds to a succinimide (*) form produced as a by-product of high-temperature reduction of RumC1hm before iodoalkylation. (**D**) Identification of bridging partners. (**E**) Double-hairpin–like structure of mRumC1. Cysteine residues bridged via thioether bonds are shown in purple, and their amino acid partners are indicated in orange.

including HNCACB, CBCA(CO)NH, HNCA, HN(CO)CA, HNCO, and HN(CA)CO. The chemical shifts of the α-carbons of A12, N16, R34, and K42 were found at 72.2, 68.6, 74.5, and 75.5 parts per million (ppm), respectively (fig. S6A). These values are 15 ppm downfield compared to the average value observed for unmodified residues. This is consistent with the influence of an electronegative atom, such as sulfur, being directly attached. Similar chemical shifts were reported for the modified α-carbon atoms in subtilosin A, thurincin H, and thuricin CD (*6*–*9*, *39*). Analyses of the total correlation spectroscopy (TOCSY) and ^{13}C TOCSY-HSQC experiments confirmed that A12, N16, R34, and K42 α-carbons are fully substituted, with no α-protons attached. The atomic connectivity of each thioether linkage was determined by analyzing the nuclear Overhauser effect spectroscopy (NOESY) and ^{15}N NOESY-HSQC data, which show through-space interactions between protons that are close to each other. Nuclear Overhauser effect (NOE) interactions were observed between the β-protons of C3 and the amide proton (HN) of N16, the β-protons of C5 and the HN proton of A12, and the β-protons of C22 and the HN proton of K42 (fig. S6B). These NOE data assigned unambiguously three of the four thioether linkages between C3 and N16, C5 and A12, and C22 and K42. The fourth linkage is not evident to be assigned because of C26 unresolved peak, but only this Cys residue remains to form a thioether bridge with the α-carbon atom of R34 in mRumC1.

Sequential proteolytic cleavage of mRumC1 is required to produce an active form

As we established that in vivo RumC1 and mRumC1 retain the same posttranslational modifications, we performed all subsequent antimicrobial assays using mRumC1. Similar to the chemically synthesized, unmodified form of RumC1, mRumC1 had no anti-*Cp* activity, suggesting that the presence of intramolecular thioether bonds is not sufficient to produce antimicrobial activity (fig. S7A). As a protective strategy for the organisms producing them, RiPPs are in an inactive state until their leader peptide is released as proposed by Yang and van der Donk (*40*). We therefore decided to remove the leader peptide from mRumC1. After checking the up-regulation of the corresponding mRNA by quantitative reverse transcription polymerase chain reaction in the cecal contents (fig. S3A), we cloned the *rumPc* gene encoding the putative leader metallopeptidase identified in the *rumC*-regulon to overproduce and purify the recombinant RumPc protein (fig. S3, B and C, bottom). RumPc-treated mRumC1 (i.e., mRumC1c) remained inactive against *Cp* (fig. S7C, top). Moreover, RP-C18 and LC-MS analyses revealed that mRumC1c retains the FEGSK amino acid motif in its N terminus unlike native RumC1 obtained from rat feces (Figs. 2D and 3A and fig. S7, B and C). Because Ramare and co-workers (*17*) previously reported a trypsin-dependent anti-*Cp* activity in the cecal contents, we next performed proteolytic digestion of mRumC1c by pancreatic trypsin. This sequential treatment led to the complete removal of the leader sequence and generated a mature peptide (i.e., mRumC1cc) identical to in vivo–produced RumC1, as confirmed by high-performance liquid chromatography (HPLC) and MS analyses, which was active against *Cp* (fig. S7, B and C). In good agreement with these results, direct treatment of mRumC1 with pancreatic trypsin led to the complete removal of the leader peptide sequence within 1 hour (fig. S7D). This one-step cleavage was thus subsequently used to prepare active mRumC1cc, currently renamed RumC1 (fig. S7, A, B and C).

Considering these results, the hydrophobicity profile, and the absence of any kind of signal peptide predicting a subcellular localization of RumPc, we can propose an in vivo RumC1 maturation process involving (i) an in situ posttranslational modification of the core peptide by RumMc1 followed by a partial cleavage of the leader peptide by RumPc and (ii) an ex situ cleavage of the five remaining N-terminal amino acids of the leader peptide by pancreatic trypsin, leading to an active bacteriocin released in the gut microbiome. To conclude, the intracellular RumPc cleavage followed by the extracellular trypsin cleavage to produce an active form of a sactipeptide represents a perfect example of mutualism between a symbiont and its host collaborating to generate an antipathogenic molecule as a protective strategy for both.

RumC1 is safe for use against pathogens and MDR bacteria

The antimicrobial spectrum of RumC1 was investigated on a broad range of Gram-positive and Gram-negative bacteria, including pathogens and MDR strains. For these studies, we used RumC1 produced by heterologous expression and activated by trypsin cleavage to determine minimal inhibitory concentrations (MICs; Fig. 4A). To distinguish between a bactericidal and a bacteriostatic effect, we also determined the minimal bacteriostatic concentration (MBC) for each sensitive strain (Fig. 4A). RumC1 was highly effective against a range of pathogenic *Clostridium* species with very low MIC and MBC values. An MBC value of 1.56 μM was observed against *Cp*, which is the third cause of foodborne infections in the United States after Norovirus and *Salmonella* spp. according to the Centers for Disease Control and Prevention (CDC). RumC1 is also effective against *Clostridium difficile* (6.25 μM < MBC < 12.5 μM), one of the main pathogens highlighted in the report published by the CDC in 2013 on "Antibiotic Resistance Threats in the United States" and categorized as an urgent threat for which new antibiotics are needed. Even lower MBC value (0.4 μM) was measured for *Clostridium botulinum*, a pathogen responsible for foodborne botulism (via a preformed toxin), infant botulism (intestinal infection via a toxin-forming *C. botulinum*), and wound botulism. Moreover, RumC1 was also active against a range of Gram-positive organisms such as *Staphylococcus aureus* and MDR strains such as vancomycin-resistant *Enterococcus faecalis*, nisin-resistant *Bacillus subtilis* or methicillin-resistant *S. aureus* (MRSA) at clinically relevant MIC values in the micromolar range of 0.8 to 50 μM. As expected, RumC1was also active against closely phylogenetically related bacteria such as *Clostridium coccoides* with an MIC value of 1.56. Although the antimicrobial assays were performed on a relatively exhaustive panel of bacteria, it seems that RumC1 is not active against Gram-negative bacteria, for which MICs were determined to be >100 μM (Fig. 4A). Last, except for MRSA, the MBC values were identical to the MICs, suggesting that the effect of RumC1 is bactericidal (Fig. 4A).

After assessing the activity spectrum of RumC1, we investigated its mode of action on *Cp* cells. As it is well known that many antimicrobial peptides have a pore-forming effect, we assessed the permeabilization potency of RumC1 following the fluorescent emission of *Cp* cells treated with propidium iodide (PI), a DNA intercalating agent, and the incorporation of the nucleic acid dye SYTOX Green by fluorescence microscopy. Both fluorescent compounds cannot cross undamaged membranes. We used the detergent cetyltrimethylammonium bromide (CTAB) and a well-characterized pore-forming bacteriocin, nisin, as positive controls. Even after 2 hours of treatment, cells exposed to RumC1 showed no PI nor SYTOX Green incorporation, whereas permeabilization with nisin resulted in 59% of the maximum PI incorporation measured with CTAB and caused 97% of the cells to

A

Bacteria	Strain	MIC (μM)	MBC (μM)
Clostridium perfringens	ATCC 13124	1.56	1.56
Clostridium difficile	DSMZ 1296	6.25	6.25–12.5
Clostridium botulinum	DSMZ 1985	0.4	0.4
Staphylococcus aureus	ATCC 6538P	25	25–50
Staphylococcus aureus MRSA[1]	ATCC BAA-1717	50	>100
Enterococcus faecalis VER[2]	DSMZ 13591	12.5	25
Bacillus subtilis	ATCC 6633	0.4	0.4
Bacillus subtilis NR[3]	DSMZ 347	0.8	0.8
Clostridium coccoides	ATCC 29236	1.56–3.13	1.56–3.13

[1]MRSA = methicillin-resistant *Staphylococcus aureus*, [2]VER = vancomycin-resistant, [3]NR = nisin-resistant.

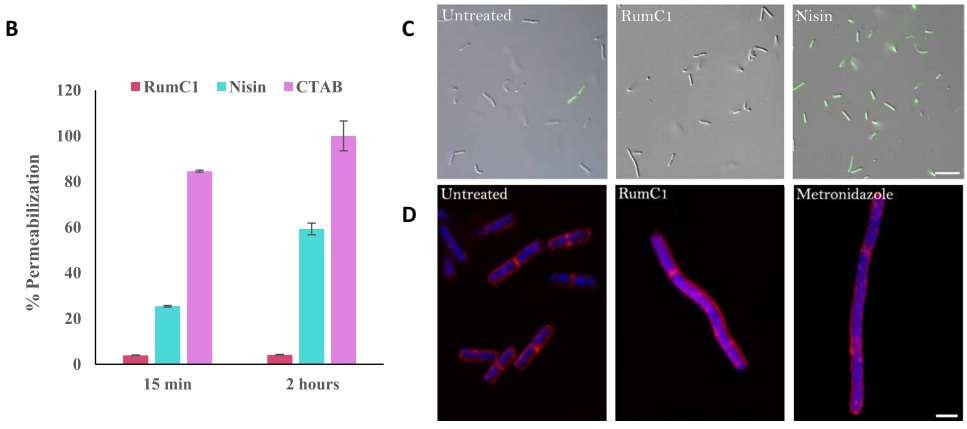

Fig. 4. RumC1 antimicrobial activity. (**A**) Activity spectrum of RumC1 against selected Gram-positive strains. MIC and MBC were >100 μM for the following Gram-negative strains tested: *Salmonella enterica* (CIP 80.39), *E. coli* (ATCC 8739), *E. coli* MR4 (DSMZ 22314), *Pseudomonas aeruginosa* (ATCC 9027), *P. aeruginosa* fluoroquinolone resistant (CIP 107398), *Acinetobacter baumanii* (CIP 103572), *A. baumanii* multiresistant (CIP 110431), and *Klebsiella pneumoniae* MR4 (DSMZ 26371). (**B** and **C**) Membrane permeabilization assay on *Cp* cells treated with RumC1 or nisin based on measurement of PI incorporation (B) or SYTOX Green staining (C). (B) Cells incubated with cetyltrimethylammonium bromide (CTAB) were used as a positive lysis control, and untreated cells were used as a negative control. (C) Cells were treated for 15 min before staining. Scale bar, 10 μm. (**D**) Confocal imaging of control *Cp* cells or *Cp* cells treated with RumC1 or metronidazole. Membranes were stained with FM4-64FX, and DNA was stained with DAPI (4′,6-diamidino-2-phenylindole). RumC1 treatment leads to three morphotypes identical to the ones induced by metronidazole (fig. S9). This figure shows one of these three morphotypes, i.e., one regular cell associated with a cell three to four times longer and with uncondensed DNA throughout the cells with a few spots of highly condensed DNA. Scale bar, 2 μm.

stain positive for SYTOX Green (Fig. 4, B and C). Accordingly, RumC1 is unable to insert into total lipids extracts obtained from *Cp* contrarily to nisin and CTAB (fig. S8). Thus, it appears that, unlike most bacteriocins targeting Gram-positive bacteria, RumC1 does not have a pore-forming action and has most likely an intracellular target. RumC1 can also be expected to be supported by an active membrane transporter to reach the intracellular compartment. Although most peptides acting on intracellular targets are usually active against Gram-negative bacteria and have a much narrower spectrum, some RiPPs such as thiopeptides have a broad spectrum and have been shown to inhibit translation in Gram-positive cells (*41*). We next tried to identify the cellular pathways inhibited by RumC1 through phenotype imaging experiments based on the "bacterial cytological profiling" method (*42*) adapted to anaerobic conditions. Membranes and DNA from *Cp* cells were stained with FM4-64FX and 4′,6-diamidino-2-phenylindole (DAPI), respectively, and confocal images were acquired. Morphological changes on *Cp* cells induced by treatment with RumC1 were compared to the phenotypes induced by conventional antibiotics with well-characterized mechanisms of action. Treatment with RumC1 produced three morphotypes affecting cell length and organization, as well as DNA condensation (Fig. 4D). No morphological similarities were observed in cultures treated either with antibiotics that inhibited transcription or cell wall synthesis or even with those causing loss of membrane potential (fig. S9, A and B). However, when cells were treated with metronidazole, an antibiotic that inhibits nucleic acid synthesis, we observed the three phenotypes identical to those induced by treatment with RumC1. How metronidazole affects nucleic acid synthesis remains unclear. Studies suggest that it could act directly on DNA and disrupt its structure. Some other studies showed that it indirectly inhibits DNA synthesis and repair systems (e.g., mismatch or SOS), possibly by disrupting the cell redox system resulting in ribonucleotide reductase inhibition (*43*). Hence, we hypothesize that RumC1 most likely inhibits nucleic acid synthesis in a metronidazole-like manner.

Antimicrobial efficiency not only must be sufficient to develop a therapeutic molecule but also must be safe for the host. We therefore assayed the cytotoxicity of RumC1 on human cells using two intestinal (Caco2 and T84) and one gastric (N87) cell lines. On the basis of their metabolic activity (via resazurin assays), RumC1 did not affect the viability of these cell lines, even at high concentrations of RumC1 [IC_{50} (median inhibitory concentration), > 200 μM; fig. S10A]. At concentrations of RumC1 up to 200 μM, metabolic activities of Caco2, N87, and T84 cells were at least 90, 80, and 70%, respectively, of the activity measured in untreated cells. Furthermore, RumC1 induced no hemolysis of human erythrocytes even at high concentrations [EC_{50} (median effective concentration), > 200 μM; fig. S10B]. Last, no resistance was induced in serial subcultures of *Cp* exposed daily to RumC1, whereas equivalent treatment with metronidazole led to the emergence of resistant bacteria with up to 500-fold higher MICs (fig. S10C). The high potency of RumC1 against pathogenic strains combined with its lack of effect on eukaryotic cells and the absence

of resistance development makes it a relevant candidate either as therapeutic agent or as food safety agent.

DISCUSSION

Through this study, we were able to (i) develop and optimize a protocol to purify a natural molecule exhibiting antibiotic activity produced by a human intestinal symbiont from cecal contents harvested from *R. gnavus* E1–monoassociated rat and (ii) produce an active recombinant form of this RiPP after maturation and sequential and controlled proteolytic cleavage to remove the leader peptide, in line with the steps naturally occurring in the human gut (Fig. 5). For almost all natural RiPPs, the precursor genes encode an unprocessed peptide bearing an N-terminal leader peptide in addition to the C-terminal core peptide. Although leader peptides have been suggested to play multiple roles during RiPPs biosynthesis, such as acting as a secretion signal or as a recognition pattern for the maturation enzymes, the protective effect of keeping the peptide inactive before secretion remains the most notable (*3*, *44*). Several studies on the broad subclasses of RiPPs, the classes II and III lantibiotics (e.g., cytolysin, plantaricin W, haloduracin, lichenicidin, carnolysin, and flavipeptin or NAI-112, respectively) have reported similarities with a two-step activation process using proteases (*45*–*51*). However, despite the five or six amino acid overhangs remaining after the first proteolytic cleavage in mRumC1c, the GG/ or GA/ recognition motif usually found in lantibiotics is not conserved in the leader peptides of RumC isoforms, in favor of an /FE pattern recognized as a cleavage site by RumPc. Broadly, the different classes of lantibiotics, namely, I, II, and III, involve subtilisin-like serine proteases, papain-like cysteine proteases, and Zn-dependent bifunctional (i.e., endo- and aminopeptidase) proteases, respectively, whereas RumPc is a monofunctional Zn-metallopeptidase with an endo-mode of action recognizing an undescribed motif (/FE) to date. In addition, the second step occurring in the maturation process of RumC1 and leading to an active form involves the human pancreatic trypsin. Consequently, we have identified a two-step cleavage process involving a monofunctional Zn-metallopeptidase from the symbiont (i.e., RumPc) and a serine protease from the host organism (i.e., trypsin) to get an active RiPPs. To our knowledge, nothing equivalent has been reported for the RiPPs, especially for the lantibiotic and sactibiotic subclasses (Fig. 5). Last, through a deep MS study on both the natural isoforms of RumC and recombinant forms, we were able to conclude that maturation of the bacteriocin involves a radical SAM sactisynthase,

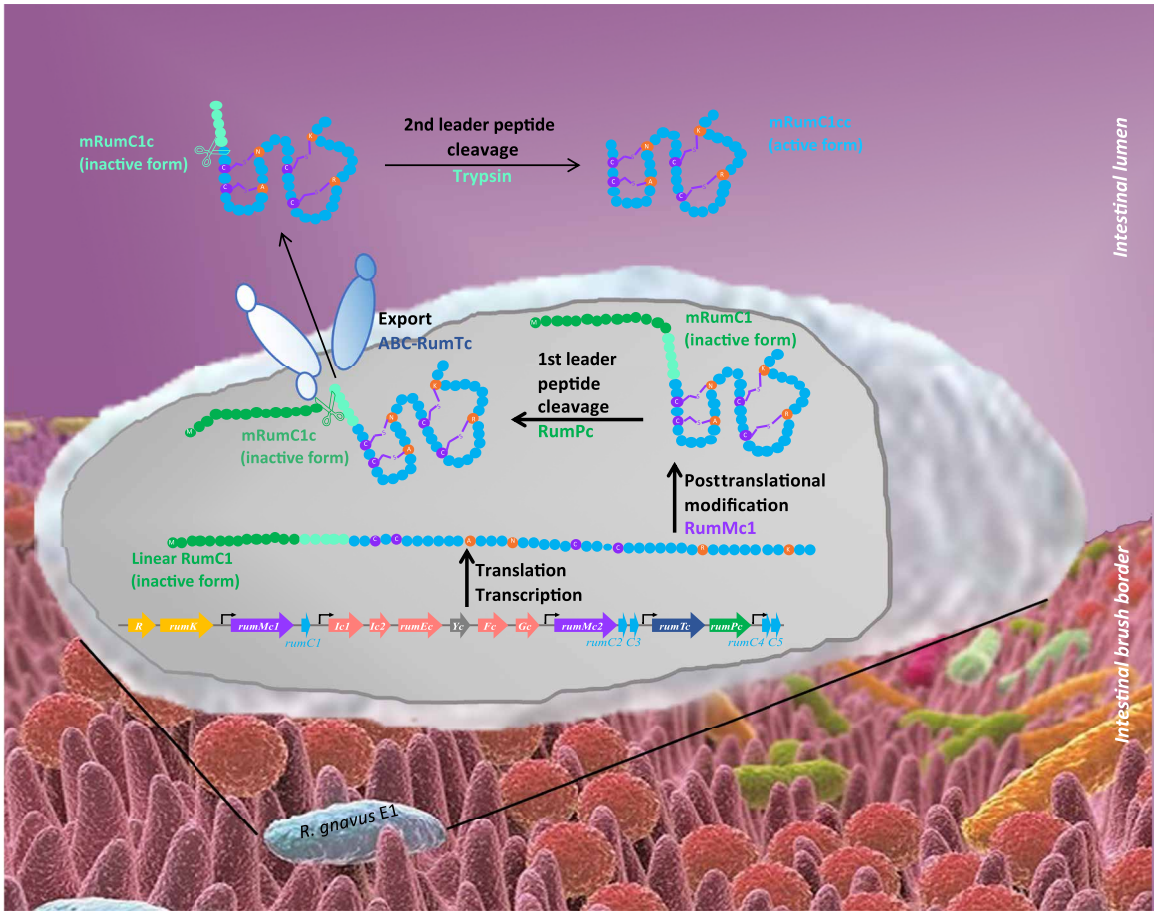

Fig. 5. Proposed mechanism of maturation and activation of RumC1 in the human gut. After induction of the two-component system, conventional transcription, and translation of the gene regulon Ruminococcins C, the intracellular RumC1 maturation process involves (i) an in situ posttranslational modification of the core peptide by RumMc1, leading to the inactive mRumC1; (ii) a partial cleavage of the leader peptide by RumPc, leading to the still inactive mRumC1c; (iii) an export in the intestinal lumen by RumTc; and (iv) an ex situ cleavage of the five remaining N-terminal amino acids of the leader peptide by pancreatic trypsin, leading to an active mRumC1cc (i.e., RumC1).

RumMc, itself capable of generating four thioether bridges resulting in a new folding pattern, which has never yet been described in the literature. The discovery of this new double-hairpin structure leads us to propose a new subclass of sactibiotics.

We thoroughly characterized the bactericidal activity of RumC1 and found that, unlike some bacteriocins (e.g., colicine), which are defined as "narrow-spectrum," RumC1 is active against not only a broad spectrum of Gram-positive bacteria, including phylogenetically *R. gnavus*–related bacteria such as *Cp*, *C. difficile*, and *C. botulinum*, but also more distant bacteria such as *S. aureus*, including MDR strains. Furthermore, our preliminary data suggest a mechanism involving inhibition of nucleic acid synthesis in a metronidazole-like manner, but additional investigation is needed to corroborate this hypothesis. As a result, MICs for RumC1 are in the micromolar range for, e.g., *C. difficile* or *Cp*. Safety assays on several human cell lines revealed no toxicity, and RumC1 does not trigger resistance development unlike many conventional antibiotics. This characteristic is essential when developing new drugs against pathogens considering the rise of MDR strains worldwide. On the basis of all these findings, it is highly relevant to consider RumC for the elaboration of therapeutic strategies, after drug optimization or in combination with other antimicrobial agents or antibiotics, for human or animal health. *Cp* is also a major pathogen affecting poultry, where it causes necrotic enteritis associated with up to 50% mortality (*52*). Consequently, *R. gnavus* E1 or other RumC-like producing bacteria could be considered as natural probiotics and administered for the prevention against Gram-positive pathogens. Otherwise, sactibiotics and other groups of bacteriocins could be helpful in combinatorial therapies with other antimicrobial agents including, e.g., antibiotics to reduce emergence of resistance or to fight clinical pathogens, and RumC1 could be considered in that way (*32*).

Last, from an ecological standpoint, the *R. gnavus* E1 and human partnership constitute a perfect example of mutualism where both host and symbiont work together and need each other to produce an active bacteriocin to fight a common enemy: an opportunistic pathogen for the host and a competitive species for the same ecological environment for the symbiont.

MATERIALS AND METHODS

Animals and sample collection

Animal experiments were performed according to the guidelines of the French Ethics Committee, i.e., agreement no. A78-322-6. Axenic male F344 M rats (6 weeks old) provided by the Germ Free Animals facility ANAXEM (Animalerie Axénique de Micalis) platform [Institut National de la Recherche Agronomique (INRA), UMR 1319 Micalis, France] and maintained on a standard diet during 12 days were inoculated with *R. gnavus* E1 [0.5 ml of late log-phase culture at 10^9 colony-forming units (CFU)/ml] by intragastric route to generate *R. gnavus* E1 monoxenic rats (n = 10). After 5 days, individual fecal samples were collected and bacterial counts were estimated by plating serial dilutions of suspensions. We plated these samples on Brain Heart Infusion agar supplemented with yeast extract (5 g/liter) and hemin (5 mg/liter) (BHI-YH), and on Luria-Bertani (LB) agar, under aerobic and anaerobic conditions, to check for the colonization by *R. gnavus* E1 and possible contamination by other bacteria. The animals were sacrificed 12 days after inoculation, and feces and cecal contents were collected. Samples were frozen in liquid nitrogen before being stored at −80°C until RNA or bacteriocin purification.

Bacteriocin purification

Cecal contents of *R. gnavus* E1 monoxenic rats were diluted in phosphate-buffered saline (PBS) (10 g for 30 ml) supplemented with a protease inhibitor cocktail (cOmplete ULTRA tablets EDTA-free, Roche). The suspension was centrifuged at 10,000*g* for 15 min. Resuspension and centrifugation were repeated twice in half the initial volume of PBS. The three supernatants were pooled and filtered on a polyethersulfone membrane with a 10-kDa cutoff (Merck). The resulting filtrate, containing small molecules including peptides, was submitted to ion exchange chromatography using a Carboxymethyl Sepharose column (GE Healthcare) at 4°C. Elution was performed at 2 ml/min with 20 mM acetate sodium buffer at pH 6.5 under isocratic conditions for 36 min, followed by a linear 0 to 0.5 M sodium chloride gradient for 60 min with a detection at 214 and 280 nm. Elution fractions were desalted by DSC-18-SPE columns (Sigma-Aldrich). Briefly, samples were loaded after dilution (1:1) in 0.1% trifluoroacetic acid (TFA), washed with 0.1% TFA, and eluted in 90% acetonitrile (ACN) and 0.1% TFA before being lyophilized and resuspended in water. Fractions displaying anti-*Cp* activity (as described below) were further purified by size exclusion chromatography using a Superdex 30 Increase column (GE Healthcare). Elution was performed at 4°C at 0.5 ml/min for 120 min under isocratic conditions with PBS, and collected fractions were desalted as described above. Active fractions were then applied to a Jupiter 15-µm C18 300 Å analytical reverse-phase HPLC column (250 mm by 21.2 mm; Phenomenex). Peptides were eluted at 1 ml/min with a 0 to 40% linear gradient of 90% ACN and 0.1% TFA for 30 min before being lyophilized and resuspended in water. The different fractions were maintained at 4°C during all purification steps and stored at −20°C. The protein concentration was estimated either by the Bradford coloration method using a bovine serum albumin standard curve or by measuring the A280 and using the theoretical extinction coefficient of 8480 M^{-1} cm^{-1}.

Bacteriocin activity assays

To track the presence of the bacteriocin along the purification, samples were tested for their antimicrobial activity against *Cp* at each step using the diffusion assay. If needed, samples were concentrated using a Speed-Vac concentrator (Thermo Fisher Scientific). A 10^{-3} dilution of an overnight culture of *Cp* strain [American Type Culture Collection (ATCC) 13124] was spread on BHI-YH agar. After drying for 30 min at room temperature, wells with a diameter of 6 mm were dug with a Pasteur pipette and 100 µl of sample was added per well. Alternatively, 10 µl was spotted directly onto the plate. The presence of inhibition halos around the samples was examined after incubation of the plates at 37°C for 24 hours under anaerobic conditions.

Expression and purification of MBP-RumC1

A synthetic plasmid containing the *E. coli* codon-optimized gene of *R. gnavus* E1 encoding RumC1 (pETM-40-*rumC1*, kanamycin resistant) was obtained from GenScript (Piscataway, NJ), which allows the expression of a MBP (maltose-binding peptide)–tagged peptide. A tobacco etch virus nuclear-inclusion-a endopeptidase (TEV protease) site was inserted in the linker between MBP and RumC1 peptide. pETM40-*rumC1* was used to transform competent *E. coli* BL21 (DE3) cells for expression. The resulting *E. coli* BL21 (DE3) strain was grown in M9 medium containing kanamycin (50 µg/ml), vitamin B1 (0.5 µg/ml), $MgSO_4$ (1 mM), and glucose (4 mg/ml) at 37°C. At an optical density (OD_{600}) of 0.8, the culture was induced using 1 mM isopropyl-β-D-thiogalactopyranoside (IPTG). The temperature was

reduced to 25°C, and the cells were grown for 15 hours under stirring. Cells were then harvested by centrifugation at 4000 rpm for 20 min at 4°C. Cell pellet was suspended in 40 ml of buffer A [50 mM tris (pH 8) and 50 mM NaCl] supplemented with one tablet of a protease inhibitor cocktail (cOmplete, EDTA-free Protease inhibitor cocktail tablets, Roche). Cell pellet was then sonicated, and the lysate was clarified by centrifugation at 40,000 rpm for 40 min at 4°C. The supernatant was collected and passed over Dextrin Sepharose High Performance columns (5 ml; MBPTrap HP, GE Healthcare) coupled to a fast protein liquid chromatography (FPLC) (ÄKTA Purifier 900, ÄKTA FPLC Systems, GE Healthcare). Columns were washed with four column volumes of buffer A. MBP-RumC1 was eluted with buffer B [50 mM tris (pH 8), 50 mM NaCl, and 40 mM maltose]. Fractions containing MBP-RumC1 were pooled and concentrated in a 30,000 molecular weight cutoff (MWCO) filter using Amicon Ultra centrifugal filter devices. The sample was digested by TEV protease for a final TEV protease:MBP-RumC1 ratio of 1:20 (w/w) and incubated for 30 min at room temperature. MBP-tag, TEV protease, and unmodified RumC1 were separated by loading over a HiLoad 16/60 Superdex 75 prep grade column (GE Healthcare) equilibrated in buffer C [50 mM Hepes and 100 mM NaCl (pH 7.5)]. The peptide concentration was estimated by ultraviolet-visible (UV-vis) spectroscopy on a Cary 50 UV-vis spectrophotometer (Varian) by using an extinction coefficient of 8480 M^{-1} cm^{-1} at 280 nm.

Heterologous expression and purification of mature mRumC1

A synthetic plasmid containing the *E. coli* codon-optimized gene of *R. gnavus* E1 encoding RumMc1 (pET-15b-*rumMc1*, ampicillin resistant) was obtained from GenScript. Plasmids pET-15b-*rumMc1*, pETM-40-*rumC1*, and psuf (chloramphenicol resistant) containing *sufABCDSE* genes were used to transform competent *E. coli* BL21 (DE3) cells for expression. The resulting strain was grown in M9 medium containing kanamycin (50 μg/ml), amp (100 μg/ml), chl (34 μg/ml), vitamin B1 (0.5 μg/ml), $FeCl_3$ (50 μM), $MgSO_4$ (1 mM), and glucose (4 mg/ml) at 37°C. At an optical density (OD_{600}) of 0.8, $FeCl_3$ (100 μM) and L-cysteine (300 μM) were added and the culture was induced using 1 mM IPTG. The temperature was reduced to 25°C, and the cells were grown for 15 hours under stirring. Cells were then harvested by centrifugation (4000 rpm for 20 min at 4°C). Mature MBP-mRumC1 was then purified as described above for unmodified RumC1.

RumPc production and purification

A synthetic plasmid containing the *E. coli* codon-optimized synthetic gene of *R. gnavus* encoding RumPc (pET-21a–*rumPc*, ampicillin-resistant) was obtained from GenScript. In silico analysis on the *rumPc*-encoding gene to identify a putative signal peptide was performed by using the SignalP 5.0 server (www.cbs.dtu.dk/services/SignalP/). The plasmid was transformed into thermo-competent BL21 (DE3) *E. coli* cells. Ampicillin-resistant colonies were isolated and subcultured in LB broth. Subcultures were used to inoculate 1 liter of terrific broth (TB) medium supplemented with ampicillin (final concentration, 100 μg/ml). The culture was initiated at OD_{600} = 0.05 in prewarmed medium and incubated at 37°C for 1.5 hours and 28°C for 40 min (until OD_{600} = 0.5). Expression was then induced using 0.5 mM IPTG, and the culture was incubated for 3.5 hours at 28°C. Cells were harvested by centrifugation (5000*g*, 20 min, 4°C) and frozen at −20°C. Cells were lysed in buffer D [50 mM NaH_2PO_4 (pH 7.5) and 150 mM NaCl] using a cell disrupter (Série TS, CellD, Constant Systems). The soluble fraction of the cell lysate was retrieved by centrifugation (14,000*g*, 30 min, 4°C) and filtered at 0.22 μm before being submitted to a 1-ml HisTrap HP purification affinity column (GE Healthcare) according to the manufacturer's instructions. RumPc was eluted using a 0 to 500 mM gradient of imidazole. Pooled fractions containing RumPc (detected by SDS–polyacrylamide gel electrophoresis) were ultrafiltered through a PES (polyethersulfone) 10-kDa MWCO membrane and washed 10 times in buffer C. The protein concentration was estimated by measuring the A280 and using an extinction coefficient of 52,425 M^{-1} cm^{-1}.

mRumC1 leader peptide cleavage

Maturated RumC1 obtained by heterologous coexpression of *rumC1* and *rumMc1* genes in *E. coli* and purified as described above was treated with either RumPc or TPCK (*N*-tosyl-L-phenylalanine chloromethyl ketone)–treated trypsin (Sigma-Aldrich) for 1 hour at 37°C. The molar ratios used were 200:1 for mRumC1:trypsin and 1:5 for mRumC1:RumPc. mRumC1c and mRumC1cc were purified using RP-C18-HPLC with the following gradient: 10 min at 22% followed by 12 min from 22 to 38% of 90% ACN and 0.1% TFA. For the preparation of large amounts of mRumC1cc for biological activity assays, mRumC1 was cleaved with trypsin and purified with the above RP-C18-HPLC conditions on a preparative column (250 mm by 21.2 mm; Phenomenex, Jupiter, 15 μm, 300 Å).

Nano–LC-MS/MS analyses

RumC fractions were generally injected at a concentration of 0.1 μM. Samples were diluted in 5% (v/v) ACN and 0.1% (v/v) TFA and analyzed by online nano–LC-MS/MS (NCS HPLC, Dionex, and Q Exactive HF, Thermo Fisher Scientific). Peptides were sampled on a 300 μm by 5 mm PepMap C18 precolumn and separated on a 75 μm by 250 mm PepMap C18 column (Dionex). The nano-LC method consisted of a 40 min gradient at a flow rate of 300 nl/min, and MS and MS/MS data were acquired using Xcalibur (Thermo Fisher Scientific). Highly sensitive method (by increasing the ion time in the trap to 200 ms) in MS/MS was used to improve the signal to noise of the fragmented large peptides. For the analysis of the maturated forms, combined high collision dissociation energies of 20 to 27 were used to promote the breaking of both weak bonds (thioether bridge) and stronger bonds (amide bonds). Both MS/MS spectra were summed up to give a combined spectrum. Parallel reaction monitoring experiments were also conducted to target the species of interest.

MS data analyses

Data were processed automatically using Mascot Distiller software (version 2.5.1, Matrix Science) followed by Mascot (version 2.6) searches using the sequences of the different peptides of interest as database. None was chosen as enzyme, and the precisions were set at 10 ppm for the peptide precursor and 20 milli mass unit for the fragments. At first instance, many different possibilities of variable modifications were tested to find out on which amino acid was observed in the dehydramino modification (−2H) (*36*). Manual annotations were performed in parallel to Mascot searches to assess the positions of thioether linkages. For final searches, dehydramino (A, N, R, and K), deamidation (NQ), and ammonia loss (N) were set as variable modifications. Qual Browser and Xtract (Thermo Fisher Scientific) were used for the display and the deconvolution of the spectra. All considered experimental masses were monoisotopic and nonprotonated masses.

Antimicrobial activity

All targeted strains were grown at 37°C in LB broth under aerobic conditions (200 rpm), except for Clostridia that were grown in BHI-YH under anaerobic conditions (in a Trexler-type anaerobic chamber, without stirring). Peptides dissolved in sterile distilled water were sterilized 2 min under UV light and added to sterile F-bottom polypropylene 96-well microplates from 100 to 0.1 μM. Twofold series dilutions were performed in cell suspension of each bacterial target, including *Cp*, at 10^{-4} OD_{600} units. For other Clostridia, higher concentrations of bacteria (i.e., cell suspensions at 10^{-3} OD_{600} units) were used. MIC was defined as the lowest concentration of peptide that inhibited the visible growth of bacteria after 24 to 48 hours incubation at 37°C. Cell suspensions were then plated on appropriate solid medium devoid of any antimicrobial agent to evaluate bacterial growth. MBCs were defined as the lowest concentration of peptide that inhibited the visible growth of bacteria after 24 to 48 hours incubation at 37°C on a solid medium. MICs and MBCs were determined three times. Sterility and growth controls were prepared for each assay.

Membrane permeability assay

Permeabilization of the bacterial membrane by RumC1 was measured using the cell-impermeable DNA/RNA probe PI as previously explained (*53*, *54*). A bacterial culture of *Cp* was grown until it reached 10^9 bacteria/ml and then centrifuged for 5 min at 300s. Bacteria pellet was then resuspended in sterile PBS in the original volume. PI (Sigma-Aldrich) was then added to the suspension at a final concentration of 60 μM. One hundred microliters of this suspension was then transferred into 96-well black plate (Greiner Bio-One) and treated with RumC1 or nisin at 5× their MIC values. Water and CTAB diluted at 300 μM final concentration were used as negative and positive controls, respectively. After 15- and 120-min incubations at 37°C under anaerobic conditions, fluorescence was measured (excitation at 530 nm and emission at 590 nm) using a microplate reader (Synergy Mx, BioTek). Results were expressed as the percentage of total permeabilization obtained by treatment with CTAB. All experiments were done in triplicate. For the permeabilization assay with SYTOX Green (Thermo Fisher Scientific), an overnight culture of *Cp* was diluted at 1:100 in BHI-YH and grown at 37°C under anaerobic conditions until OD_{600} = 0.2. Cells were then treated with RumC1 or nisin at 5× their MIC values for 15 min before being stained with SYTOX Green at 0.5 μM. Then, cells were rinsed with Hanks' balanced salt solution +/+ (Gibco) and resuspended in VECTASHIELD (Vector Laboratories, CliniSciences H-1000). Observations were lastly performed with a Leitz DMRB microscope (Leïca), equipped with a Leïca DFC 450C camera.

Study of the mode of action based on phenotype imaging by confocal microscopy

Phenotype observations by confocal microscopy were used to evaluate the mode of action of RumC1, as previously described (*42*) but with some modifications. An overnight culture of *Cp* was diluted at 1:100 in BHI-YH and grown at 37°C under anaerobic conditions until OD_{600nm} = 0.2. Bacteria were then treated with RumC1 or antibiotics with known mechanisms of action (fig. S7) at 5× their MIC values for 2 hours. Then, membranes were stained with FM4-64FX (Thermo Fisher Scientific), and DNA was stained with DAPI (Sigma-Aldrich) at final concentrations of 12 and 2 μg/ml, respectively, for 10 min on ice. Cells were then pelleted (7500 rpm, 30 s) and washed with cold PBS. Cells were fixed with 4% cold paraformaldehyde for 15 min on ice before being washed with cold PBS again. Last, cells were resuspended in VECTASHIELD, and 8 μl was transferred onto microscope glass slides. Images were collected using an IX71 FluoView confocal microscope (Olympus, Rungis, France) for DAPI laser/filter ExWave = "405"/EmWave = "461" and for FM4-64FX laser/filter ExWave = "543"/EmWave = "618."

Cytotoxic assays

The intestinal toxicity of RumC1 was evaluated on human cell lines, with NCI-N87 (ATCC CRL-5822), Caco-2 (ATCC HTB-37), and T84 (ATCC CCL-248) being used as models of human gastric, small intestinal, and colonic epithelial cells, respectively. Cells were cultured in Dulbecco's modified Eagle's medium supplemented with 10% fetal bovine serum, 1% L-glutamine, and 1% streptomycin-penicillin antibiotics (all from Invitrogen). Cells were routinely seeded and grown onto 25-cm^2 flasks maintained in a 5% CO_2 incubator at 37°C. Before cytotoxicity assay, cells grown on 25-cm^2 flasks were detached using trypsin-EDTA solution (Thermo Fisher Scientific), counted using Malassez counting chamber, and seeded into 96-well cell culture plates (Greiner Bio-One) at approximately 104 cells per well. The cells were left to reach confluence for 48 to 72 hours at 37°C in a 5% CO_2 incubator. Plates were then aspirated, and increasing concentrations of RumC1 (final concentrations ranging from 0 to 200 μM) diluted in culture medium were added to the cells for 48 hours at 37°C in a 5% CO_2 incubator. Sterile water was used as a negative control. At the end of the incubation, wells were empty and cell viability was evaluated using a resazurin-based in vitro toxicity assay kit (Sigma-Aldrich) following the manufacturer's instructions (*55*). Briefly, wells were aspirated and filled with 100 μl of diluted resazurin solution obtained by dilution of the resazurin stock solution (1:100) in sterile PBS containing calcium and magnesium [PBS++ (pH 7.4), Thermo Fisher Scientific]. After 4 hours of incubation at 37°C, fluorescence intensity was measured using a microplate reader (Synergy Mx, BioTek) with an excitation wavelength of 530 nm and an emission wavelength of 590 nm. The fluorescence values were normalized by the control and expressed as the percentage of cell viability. All experiments were done in triplicate.

Hemolytic activity assay

The hemolytic activity of RumC1 was evaluated as previously described (*53*, *56*, *57*). Briefly, human erythrocytes (obtained from DivBioScience, NL) were pelleted by centrifugation at 800*g* for 5 min. Cell pellet was then resuspended in sterile PBS and centrifuged at 800*g* for 5 min. This step was repeated three times, and erythrocytes were lastly resuspended in PBS at a concentration of 8%. One hundred microliters were then added per well of sterile 96-well microplates (Greiner Bio-One) containing 100 μl of PBS with increasing concentrations of RumC1 (final concentrations ranging from 0 to 200 μM) obtained by twofold serial dilutions. Sterile water and Triton X-100 diluted in PBS at 0.1% (v/v) were used as negative and positive controls, respectively. After 1 hour at 37°C, the microplates were centrifuged at 800*g* for 5 min. One hundred microliters of cell supernatants was collected and transferred to a new 96-well microplate, and OD_{405nm} was measured using a microplate reader (Synergy Mx, BioTek). Hemolysis caused by RumC1 was expressed as the percentage of total hemolysis given by treatment with Triton X-100 at 0.1%. All experiments were done in triplicate.

Induction of resistance

Cp cells were incubated with RumC1 or metronidazole as described above for MIC determination. After 24 hours of incubation, the well

with the highest concentration of peptide or antibiotic showing visible growth was used to inoculate a new culture that was then treated again. These steps were repeated daily for 30 days to follow MIC changes.

SUPPLEMENTARY MATERIALS

Supplementary material for this article is available at http://advances.sciencemag.org/cgi/content/full/5/9/eaaw9969/DC1

Supplementary Methods

Fig. S1. Multi-alignment of RumMc radical SAM enzymes.

Fig. S2. Tandem mass spectra of RumC2-5 purified from cecal contents.

Fig. S3. Gene expression in the gut of rats monoassociated with *R. gnavus* E1 and heterologous expression and purification of MBP-mRumC1, mRumC1, and RumPc.

Fig. S4. Tandem mass spectra of N- and C-terminal fragments of RumC1 peptide present in in vivo and in vitro samples.

Fig. S5. Tandem mass spectra of mRumC1 mutants from which the residues involved in each thioether bridge were attributed.

Fig. S6. Determination of the connectivity of the thioether linkages in RumC1 by NMR.

Fig. S7. Cleavage of the leader N-terminal peptides of mRumC1 and anti-*Cp* activity assays.

Fig. S8. Evaluation of the ability of RumC1 to insert into bacterial lipids.

Fig. S9. Bacterial cytological profiling against *Cp*.

Fig. S10. Assessing RumC1 safety.

Table S1. Theoretical and experimental spectra lists.

References (*58*, *59*)

REFERENCES AND NOTES

1. A. J. O'Neill, New antibacterial agents for treating infections caused by multi-drug resistant Gram-negative bacteria. *Expert Opin. Investig. Drugs* **17**, 297–302 (2008).
2. J. O'Neill, *Tackling Drug-Resistant Infections Globally: Final Report and Recommendations* (Review on Antimicrobial Resistance, 2016).
3. P. G. Arnison, M. J. Bibb, G. Bierbaum, A. A. Bowers, T. S. Bugni, G. Bulaj, J. A. Camarero, D. J. Campopiano, G. L. Challis, J. Clardy, P. D. Cotter, D. J. Craik, M. Dawson, E. Dittmann, S. Donadio, P. C. Dorrestein, K.-D. Entian, M. A. Fischbach, J. S. Garavelli, U. Göransson, C. W. Gruber, D. H. Haft, T. K. Hemscheidt, C. Hertweck, C. Hill, A. R. Horswill, M. Jaspars, W. L. Kelly, J. P. Klinman, O. P. Kuipers, A. J. Link, W. Liu, M. A. Marahiel, D. A. Mitchell, G. N. Moll, B. S. Moore, R. Müller, S. K. Nair, I. F. Nes, G. E. Norris, B. M. Olivera, H. Onaka, M. L. Patchett, J. Piel, M. J. T. Reaney, S. Rebuffat, R. P. Ross, H.-G. Sahl, E. W. Schmidt, M. E. Selsted, K. Severinov, B. Shen, K. Sivonen, L. Smith, T. Stein, R. D. Süssmuth, J. R. Tagg, G.-L. Tang, A. W. Truman, J. C. Vederas, C. T. Walsh, J. D. Walton, S. C. Wenzel, J. M. Willey, W. A. van der Donk, Ribosomally synthesized and post-translationally modified peptide natural products: Overview and recommendations for a universal nomenclature. *Nat. Prod. Rep.* **30**, 108–160 (2013).
4. M. C. Rea, R. P. Ross, P. D. Cotter, C. Hill, Classification of bacterocins from Gram-positive bacteria, in *Prokaryotic Antimicrobial Peptides: From genes to Applications*, D. Drider, S. Rebuffat, Eds. (Springer, 2011), pp. 29–53.
5. H. Mathur, M. C. Rea, P. D. Cotter, C. Hill, R. P. Ross, The sactibiotic subclass of bacteriocins: An update. *Curr. Protein Pept. Sci.* **16**, 549–558 (2015).
6. K. Kawulka, T. Sprules, R. T. McKay, P. Mercier, C. M. Diaper, P. Zuber, J. C. Vederas, Structure of subtilosin A, an antimicrobial peptide from *Bacillus subtilis* with unusual posttranslational modifications linking cysteine sulfurs to α-carbons of phenylalanine and threonine. *J. Am. Chem. Soc.* **125**, 4726–4727 (2003).
7. K. E. Kawulka, T. Sprules, C. M. Diaper, R. M. Whittal, R. T. McKay, P. Mercier, P. Zuber, J. C. Vederas, Structure of subtilosin A, a cyclic antimicrobial peptide from *Bacillus subtilis* with unusual sulfur to α-carbon cross-links: Formation and reduction of α-thio-α-amino acid derivatives. *Biochemistry* **43**, 3385–3395 (2004).
8. M. C. Rea, C. S. Sit, E. Clayton, P. M. O'Connor, R. M. Whittal, J. Zheng, J. C. Vederas, R. P. Ross, C. Hill, Thuricin CD, a posttranslationally modified bacteriocin with a narrow spectrum of activity against *Clostridium difficile*. *Proc. Natl. Acad. Sci. U.S.A.* **107**, 9352–9357 (2010).
9. C. S. Sit, M. J. van Belkum, R. T. McKay, R. W. Worobo, J. C. Vederas, The 3D solution structure of thurincin H, a bacteriocin with four sulfur to α-carbon crosslinks. *Angew. Chem. Int. Ed. Engl.* **50**, 8718–8721 (2011).
10. W.-T. Liu, Y.-L. Yang, Y. Xu, A. Lamsa, N. M. Haste, J. Y. Yang, J. Ng, D. Gonzalez, C. D. Ellermeier, P. D. Straight, P. A. Pevzner, J. Pogliano, V. Nizet, K. Pogliano, P. C. Dorrestein, Imaging mass spectrometry of intraspecies metabolic exchange revealed the cannibalistic factors of Bacillus subtilis. *Proc. Natl. Acad. Sci. U.S.A.* **107**, 16286–16290 (2010).
11. N. A. Bruender, J. Wilcoxen, R. D. Britt, V. Bandarian, Biochemical and spectroscopic characterization of a radical *S*-adenosyl-L-methionine enzyme involved in the formation of a peptide thioether cross-link. *Biochemistry* **55**, 2122–2134 (2016).
12. T. L. Grove, P. M. Himes, S. Hwang, H. Yumerefendi, J. B. Bonanno, B. Kuhlman, S. C. Almo, A. A. Bowers, Structural insights into thioether bond formation in the biosynthesis of sactipeptides. *J. Am. Chem. Soc.* **139**, 11734–11744 (2017).
13. G. A. Hudson, D. A. Mitchell, RiPP antibiotics: Biosynthesis and engineering potential. *Curr. Opin. Microbiol.* **45**, 61–69 (2018).
14. M. G. Lamarche, B. L. Wanner, S. Crépin, J. Harel, The phosphate regulon and bacterial virulence: A regulatory network connecting phosphate homeostasis and pathogenesis. *FEMS Microbiol. Rev.* **32**, 461–473 (2008).
15. A. Pujol, E. H. Crost, G. Simon, V. Barbe, D. Vallenet, A. Gomez, M. Fons, Characterization and distribution of the gene cluster encoding RumC, an anti-*Clostridium perfringens* bacteriocin produced in the gut. *FEMS Microbiol. Ecol.* **78**, 405–415 (2011).
16. N. D. Rawlings, A. J. Barrett, P. D. Thomas, X. Huang, A. Bateman, R. D. Finn, The MEROPS database of proteolytic enzymes, their substrates and inhibitors in 2017 and a comparison with peptidases in the PANTHER database. *Nucleic Acids Res.* **46**, D624–D632 (2018).
17. F. Ramare, J. Nicoli, J. Dabard, T. Corring, M. Ladire, A. M. Gueugneau, P. Raibaud, Trypsin-dependent production of an antibacterial substance by a human Peptostreptococcus strain in gnotobiotic rats and in vitro. *Appl. Environ. Microbiol.* **59**, 2876–2883 (1993).
18. E. H. Crost, E. H. Ajandouz, C. Villard, P. A. Geraert, A. Puigserver, M. Fons, Ruminococcin C, a new anti-*Clostridium perfringens* bacteriocin produced in the gut by the commensal bacterium *Ruminococcus gnavus* E1. *Biochimie* **93**, 1487–1494 (2011).
19. E. H. Crost, A. Pujol, M. Ladiré, J. Dabard, P. Raibaud, J. P. Carlier, M. Fons, Production of an antibacterial substance in the digestive tract involved in colonization-resistance against *Clostridium perfringens*. *Anaerobe* **16**, 597–603 (2010).
20. L. Flühe, M. A. Marahiel, Radical *S*-adenosylmethionine enzyme catalyzed thioether bond formation in sactipeptide biosynthesis. *Curr. Opin. Chem. Biol.* **17**, 605–612 (2013).
21. J. B. Broderick, B. R. Duffus, K. S. Duschene, E. M. Shepard, Radical *S*-adenosylmethionine enzymes. *Chem. Rev.* **114**, 4229–4317 (2014).
22. T. A. J. Grell, P. J. Goldman, C. L. Drennan, SPASM and twitch domains in *S*-adenosylmethionine (SAM) radical enzymes. *J. Biol. Chem.* **290**, 3964–3971 (2015).
23. L. Flühe, T. A. Knappe, M. J. Gattner, A. Schäfer, O. Burghaus, U. Linne, M. A. Marahiel, The radical SAM enzyme AlbA catalyzes thioether bond formation in subtilosin A. *Nat. Chem. Biol.* **8**, 350–357 (2012).
24. B. M. Wieckowski, J. D. Hegemann, A. Mielcarek, L. Boss, O. Burghaus, M. A. Marahiel, The PqqD homologous domain of the radical SAM enzyme ThnB is required for thioether bond formation during thurincin H maturation. *FEBS Lett.* **589**, 1802–1806 (2015).
25. L. Flühe, O. Burghaus, B. M. Wieckowski, T. W. Giessen, U. Linne, M. A. Marahiel, Two [4Fe-4S] clusters containing radical SAM enzyme SkfB catalyze thioether bond formation during the maturation of the sporulation killing factor. *J. Am. Chem. Soc.* **135**, 959–962 (2013).
26. N. A. Bruender, V. Bandarian, SkfB abstracts a hydrogen atom from Cα on SkfA to initiate thioether cross-link formation. *Biochemistry* **55**, 4131–4134 (2016).
27. L. M. Walker, W. M. Kincannon, V. Bandarian, S. J. Elliott, Deconvoluting the reduction potentials for the three [4Fe-4S] clusters in an AdoMet radical SCIFF maturase. *Biochemistry* **57**, 6050–6053 (2018).
28. W. M. Kincannon, N. A. Bruender, V. Bandarian, A radical clock probe uncouples H atom abstraction from thioether cross-link formation by the radical *S* -adenosyl- l -methionine enzyme SkfB. *Biochemistry* **57**, 4816–4823 (2018).
29. T. A. J. Grell, W. M. Kincannon, N. A. Bruender, E. J. Blaesi, C. Krebs, V. Bandarian, C. L. Drennan, Structural and spectroscopic analyses of the sporulation killing factor biosynthetic enzyme SkfB, a bacterial AdoMet radical sactisynthase. *J. Biol. Chem.* **293**, 17349–17361 (2018).
30. A. Benjdia, C. Balty, O. Berteau, Radical SAM enzymes in the biosynthesis of ribosomally synthesized and post-translationally modified peptides (RiPPs). *Front. Chem.* **5**, 87 (2017).
31. A. Benjdia, A. Guillot, B. Lefranc, H. Vaudry, J. Leprince, O. Berteau, Thioether bond formation by SPASM domain radical SAM enzymes: Cα H-atom abstraction in subtilosin A biosynthesis. *Chem. Commun. Camb. Engl.* **52**, 6249–6252 (2016).
32. H. Mathur, V. Fallico, P. M. O'Connor, M. C. Rea, P. D. Cotter, C. Hill, R. P. Ross, Insights into the mode of action of the sactibiotic thuricin CD. *Front. Microbiol.* **8**, 696 (2017).
33. G. Wang, D. C. Manns, G. K. Guron, J. J. Churey, R. W. Worobo, Large-scale purification, characterization, and spore outgrowth inhibitory effect of thurincin H, a bacteriocin produced by *Bacillus thuringiensis* SF361. *Probiotics Antimicrob. Proteins.* **6**, 105–113 (2014).
34. C. E. Shelburne, F. Y. An, V. Dholpe, A. Ramamoorthy, D. E. Lopatin, M. S. Lantz, The spectrum of antimicrobial activity of the bacteriocin subtilosin A. *J. Antimicrob. Chemother.* **59**, 297–300 (2006).
35. J. E. González-Pastor, E. C. Hobbs, R. Losick, Cannibalism by sporulating bacteria. *Science* **301**, 510–513 (2003).
36. C. T. Lohans, J. C. Vederas, Structural characterization of thioether-bridged bacteriocins. *J. Antibiot.* **67**, 23–30 (2014).

37. P. M. Himes, S. E. Allen, S. Hwang, A. A. Bowers, Production of Sactipeptides in *Escherichia coli*: Probing the substrate promiscuity of subtilosin a biosynthesis. *ACS Chem. Biol.* **11**, 1737–1744 (2016).
38. B. Roche, L. Aussel, B. Ezraty, P. Mandin, B. Py, F. Barras, Iron/sulfur proteins biogenesis in prokaryotes: Formation, regulation and diversity. *Biochim. Biophys. Acta* **1827**, 455–469 (2013).
39. C. S. Sit, R. T. McKay, C. Hill, R. P. Ross, J. C. Vederas, The 3D structure of thuricin CD, a two-component bacteriocin with cysteine sulfur to α-carbon cross-links. *J. Am. Chem. Soc.* **133**, 7680–7683 (2011).
40. X. Yang, W. A. van der Donk, Ribosomally synthesized and post-translationally modified peptide natural products: New insights into the role of leader and core peptides during biosynthesis. *Chem. A Eur. J.* **19**, 7662–7677 (2013).
41. M. C. Bagley, J. W. Dale, E. A. Merritt, X. Xiong, Thiopeptide antibiotics. *Chem. Rev.* **105**, 685–714 (2005).
42. P. Nonejuie, M. Burkart, K. Pogliano, J. Pogliano, Bacterial cytological profiling rapidly identifies the cellular pathways targeted by antibacterial molecules. *Proc. Natl. Acad. Sci. U.S.A.* **110**, 16169–16174 (2013).
43. S. A. Dingsdag, N. Hunter, Metronidazole: An update on metabolism, structure-cytotoxicity and resistance mechanisms. *J. Antimicrob. Chemother.* **73**, 265–279 (2018).
44. T. J. Oman, W. A. van der Donk, Follow the leader: The use of leader peptides to guide natural product biosynthesis. *Nat. Chem. Biol.* **6**, 9–18 (2010).
45. M. C. Booth, C. P. Bogie, H. G. Sahl, R. J. Siezen, K. L. Hatter, M. S. Gilmore, Structural analysis and proteolytic activation of Enterococcus faecalis cytolysin, a novel lantibiotic. *Mol. Microbiol.* **21**, 1175–1184 (1996).
46. A. L. McClerren, L. E. Cooper, C. Quan, P. M. Thomas, N. L. Kelleher, W. A. van der Donk, Discovery and in vitro biosynthesis of haloduracin, a two-component lantibiotic. *Proc. Natl. Acad. Sci. U.S.A.* **103**, 17243–17248 (2006).
47. M. Begley, P. D. Cotter, C. Hill, R. P. Ross, Identification of a novel two-peptide lantibiotic, lichenicidin, following rational genome mining for LanM proteins. *Appl. Environ. Microbiol.* **75**, 5451–5460 (2009).
48. S. Chen, B. Xu, E. Chen, J. Wang, J. Lu, S. Donadio, H. Ge, H. Wang, Zn-dependent bifunctional proteases are responsible for leader peptide processing of class III lanthipeptides. *Proc. Natl. Acad. Sci. U.S.A.* **116**, 2533–2538 (2019).
49. G. H. Völler, B. Krawczyk, P. Ensle, R. D. Süssmuth, Involvement and unusual substrate specificity of a prolyl oligopeptidase in class III lanthipeptide maturation. *J. Am. Chem. Soc.* **135**, 7426–7429 (2013).
50. C. T. Lohans, J. L. Li, J. C. Vederas, Structure and biosynthesis of carnolysin, a homologue of enterococcal cytolysin with D-amino acids. *J. Am. Chem. Soc.* **136**, 13150–13153 (2014).
51. H. Holo, Z. Jeknic, M. Daeschel, S. Stevanovic, I. F. Nes, Plantaricin W from *Lactobacillus plantarum* belongs to a new family of two-peptide lantibiotics. *Microbiology* **147**, 643–651 (2001).
52. F. V. Immerseel, J. D. Buck, F. Pasmans, G. Huyghebaert, F. Haesebrouck, R. Ducatelle, *Clostridium* perfringensin poultry: An emerging threat for animal and public health. *Avian Pathol.* **33**, 537–549 (2004).
53. L. B. Oyama, S. E. Girdwood, A. R. Cookson, N. Fernandez-Fuentes, F. Privé, H. E. Vallin, T. J. Wilkinson, P. N. Golyshin, O. V. Golyshina, R. Mikut, K. Hilpert, J. Richards, M. Wootton, J. E. Edwards, M. Maresca, J. Perrier, F. T. Lundy, Y. Luo, M. Zhou, M. Hess, H. C. Mantovani, C. J. Creevey, S. A. Huws, The rumen microbiome: An underexplored resource for novel antimicrobial discovery. *NPJ Biofilms Microbiomes.* **3**, 33 (2017).
54. E. Di Pasquale, C. Salmi-Smail, J.-M. Brunel, P. Sanchez, J. Fantini, M. Maresca, Biophysical studies of the interaction of squalamine and other cationic amphiphilic molecules with bacterial and eukaryotic membranes: Importance of the distribution coefficient in membrane selectivity. *Chem. Phys. Lipids* **163**, 131–140 (2010).
55. C. Borie, S. Mondal, T. Arif, M. Briand, H. Lingua, F. Dumur, D. Gigmes, P. Stocker, B. Barbarat, V. Robert, C. Nicoletti, D. Olive, M. Maresca, M. Nechab, Enediynes bearing polyfluoroaryl sulfoxide as new antiproliferative agents with dual targeting of microtubules and DNA. *Eur. J. Med. Chem.* **148**, 306–313 (2018).
56. A. Tardy, J.-C. Honoré, J. Tran, D. Siri, V. Delplace, I. Bataille, D. Letourneur, J. Perrier, C. Nicoletti, M. Maresca, C. Lefay, D. Gigmes, J. Nicolas, Y. Guillaneuf, Radical copolymerization of vinyl ethers and cyclic ketene acetals as a versatile platform to design functional polyesters. *Angew. Chem. Int. Ed.* **56**, 16515–16520 (2017).
57. B. T. Benkhaled, S. Hadiouch, H. Olleik, J. Perrier, C. Ysacco, Y. Guillaneuf, D. Gigmes, M. Maresca, C. Lefay, Elaboration of antimicrobial polymeric materials by dispersion of well-defined amphiphilic methacrylic SG1-based copolymers. *Polym. Chem.* **9**, 3127–3141 (2018).
58. K. J. Livak, T. D. Schmittgen, Analysis of relative gene expression data using real-time quantitative PCR and the $2^{-\Delta\Delta CT}$ Method. *Methods* **25**, 402–408 (2001).
59. W. C. Chan, P. D. White, *Fmoc solid phase peptide synthesis: A practical approach* (Oxford University Press, 2000).

Acknowledgments: We would like to thank the people from the AVB platform (iSm2 CNRS, UMR 7313, Marseille) and the "ANAXEM platform" animal facility (Micalis INRA Jouy en Josas, France). We are indebted to S. Rabot (INRA) for providing the axenic and monoassociated rats and A. Balvay for skillful technical assistance. **Funding:** This study was supported by grants from the French National Agency for Research ("Agence Nationale de la Recherche") through the "Projet de Recherche Collaboratif" (RUMBA project, ANR-15-CE21-0020), the "Investissement d'Avenir Infrastructures Nationales en Biologie et Santé" programme (ProFI project, ANR-10-INBS-08), and partial financial support from the Labex ARCANE and CBH-EUR-GS (ANR-17-EURE-0003). We are grateful to Adisseo France company and the Association Nationale Recherche Technologie (ANRT) for funding the doctoral fellowship of C.R. entitled "Bacteriocins RumC, a novel antimicrobial peptide family as alternative to conventional antibiotics." This grant numbered Convention Industrielle de Formation par la RecherchE (CIFRE) no. 2016/0657 runs from 1 March 2017 to 1 March 2020. **Author contributions:** S.C., C.R., C.L., C.B., D.A., O.B., and S.T. performed the in vitro and in vivo assays for RumC1, RumMc1, and RumPc and were involved in interpreting the data and writing the manuscript. S.K.-J. and Y.C. performed the nano–LC-MS/MS characterizations and were involved in writing the manuscript. H.O. and M.M. performed the cytoxicity assays. C.N. performed the confocal microscopy experiments. O.I. and R.H. performed the peptide chemical synthesis. T.G., E.D., F.G., and M.F. were involved in the study design. M.A., M.L., J.P., and V.D. conceptualized the study, designed the experiments, and wrote the manuscript. **Competing interests:** The authors declare that they have no competing interests. **Data and materials availability:** All data needed to evaluate the conclusions in the paper are present in the paper and/or the Supplementary Materials. Additional data related to this paper may be requested from authors.

Submitted 13 February 2019
Accepted 27 August 2019
Published 25 September 2019
10.1126/sciadv.aaw9969

Citation: S. Chiumento, C. Roblin, S. Kieffer-Jaquinod, S. Tachon, C. Leprètre, C. Basset, D. Aditiyarini, H. Olleik, C. Nicoletti, O. Bornet, O. Iranzo, M. Maresca, R. Hardré, M. Fons, T. Giardina, E. Devillard, F. Guerlesquin, Y. Couté, M. Atta, J. Perrier, M. Lafond, V. Duarte, Ruminococcin C, a promising antibiotic produced by a human gut symbiont. *Sci. Adv.* **5**, eaaw9969 (2019).

ScienceAdvances

Ruminococcin C, a promising antibiotic produced by a human gut symbiont

Steve Chiumento, Clarisse Roblin, Sylvie Kieffer-Jaquinod, Sybille Tachon, Chloé Leprètre, Christian Basset, Dwi Aditiyarini, Hamza Olleik, Cendrine Nicoletti, Olivier Bornet, Olga Iranzo, Marc Maresca, Renaud Hardré, Michel Fons, Thierry Giardina, Estelle Devillard, Françoise Guerlesquin, Yohann Couté, Mohamed Atta, Josette Perrier, Mickael Lafond and Victor Duarte

Sci Adv **5** (9), eaaw9969.
DOI: 10.1126/sciadv.aaw9969